

Electronic Supporting Information

Optical Properties of Photodynamic Therapy Drugs in Different Environments: The Paradigmatic Case of Temoporfin

Busenur Aslanoglu,^a Ilya Yakavets,^{b,c,d} Vladimir Zorin,^{b,e} Henri-Pierre Lassalle,^{c,d} Francesca

Ingrosso,^f Antonio Monari,^{f,*} Saron Catak^{a,*}

^a*Bogazici University, Department of Chemistry, Bebek 34342, Istanbul, Turkey.*

^b*Laboratory of Biophysics and Biotechnology, Belarussian State University, Minsk, Belarus.* ^c*Université de Lorraine and CNRS, CRAN, UMR 7039, F-5400, Nancy, France.*

^d*Université de Lorraine, Institut de Cancérologie de Lorraine, F-54000, Nancy, France.*

^e*International Sakharov Environmental Institute, Minsk, Belarus.*

^f*Université de Lorraine and CNRS, LPCT, UMR 7019, F-54000, Nancy, France.*

Computational Methodology Details

Temoporfin (mTHPC) was studied in vacuo and in different environments: in water, complexed with two trimethyl- β -cyclodextrins (TM- β -CDs) and immersed in water, and next to a 1-palmitoyl-2-oleyl-sn-glycero-3-phosphocholine (POPC) lipid bilayer in contact with water. Classical Molecular Dynamics (MD) and hybrid Quantum Mechanics/Molecular Mechanics (QM/MM MD)¹ simulations were performed, the details of which is resumed in Table S1 and described in the Sections below. For the classical force field of Temoporfin, we used both a force field stemming from the application of the Antechamber protocol in the Amber Tools² with no ad hoc correction (oldFF) and a force field modified after a careful reparameterization for the torsion potential of the dihedrals of the phenol units (newFF). The dihedral angle distribution reported in the following were drawn using the VMD 1.9.3 program package.³ The Cartesian coordinates of some optimized structures are reported at the end of the report. From now on, we shall use the following scheme to refer to different simulation conditions:

Simulation 1: a) QMMD simulation of mTHPC in vacuo, **b)** QM/MMMD of mTHPC in water, **c)** QM/MM MD simulation of the 1:2 mTHPC:TM- β -CD complex in water.

Simulation 2: Classical MD simulations using oldFF for **a)** mTHPC in vacuo, **b)** mTHPC in water, **c)** 1:2 mTHPC:TM- β -CD complex in water, **d)** mTHPC next to a POPC membrane in contact with water.

Simulation 3: Classical MD simulations using newFF for **a)** mTHPC in vacuo, **b)** mTHPC in water, **c)**

1:2 mTHPC:TM- β -CD complex in water, **d**) mTHPC next to a POPC membrane in contact with water.

Table S1. Classical MD simulation and Quantum Mechanics MD simulation details of mTHPC photosensitizer in the different environments.

a) mTHPC in vacuo

	Simulation 1	Simulation 2	Simulation 3
Method	QM MD 6-31G/B3LYP	Classical MD	Classical MD
Time (ps,ns)	60ps	100 ns	100ns
Timestep (fs)	0.5	2.0	2.0
Temperature (K)	300	300	300
Ensemble	NPT	NPT Nosé-Hoover Langevin barostat^{4,5} Langevin thermostat⁶	NPT Nosé-Hoover Langevin barostat Langevin thermostat

b) mTHPC in water

	Simulation 1	Simulation 2	Simulation 3
Method	QM/MM MD 6-31G/B3LYP	Classical MD	Classical MD
Time (ps,ns)	60ps	100ns	100ns
Box size (Å)	35.0 35.2 31.3	34.9 34.2 28.1	35.0 35.2 31.3
Timestep (fs)	0.5	2.0	2.0
Temperature (K)	300	300	300
Ensemble	NPT	NPT Nosé-Hoover Langevin barostat Langevin thermostat	NPT Nosé-Hoover Langevin barostat Langevin thermostat

c) mTHPC:TM-β-CD complex in water

	Simulation 1	Simulation 2	Simulation 3
Method	QM/MM MD 6-31G/B3LYP	-	Classical MD
Time (ps,ns)	10ps	-	100ns
Box size (Å)	90.3 84.3 84.4	-	90.3 84.3 84.4
Timestep (fs)	0.0005	-	2.0
Temperature (K)	300	-	300
Ensemble	NPT	-	NPT Nosé-Hoover Langevin barostat Langevin thermostat

d) mTHPC:POPC in water

	Simulation 1	Simulation 2	Simulation 3
Method	-	-	Classical MD
Time (ns)	-	-	100 ns
Box size (Å)	-	-	81.0 81.0 138.0
Timestep (fs)	-	-	2.0
Temperature (K)	-	-	300
Ensemble	-	-	NPT Nosé-Hoover Langevin barostat Langevin thermostat

a) mTHPC in vacuo

As we mentioned above, a preliminary parametrization of the force field of mTHPC (oldFF) was performed using Antechamber and the Generalized Amber Force Field (GAFF).⁷ Classical MD simulations were performed with the NAMD⁸ program package for isolated mTHPC in order to determine possible conformations of Temoporfin and crucial interactions between its atoms. To perform a more detailed study of the conformational degrees of freedom of the molecule, quantum chemistry calculations were performed at the M062X/6-31+G(d)⁹ level of theory using the Gaussian 09 program package.¹⁰ For accuracy, polarization function is added to all heavy atoms to investigate conformations of temoporfin. The relevant degree of freedom to be studied, namely the full rotation of the dihedral angles of phenyl rings (defined in Figure S1) is reported in Figure S2.

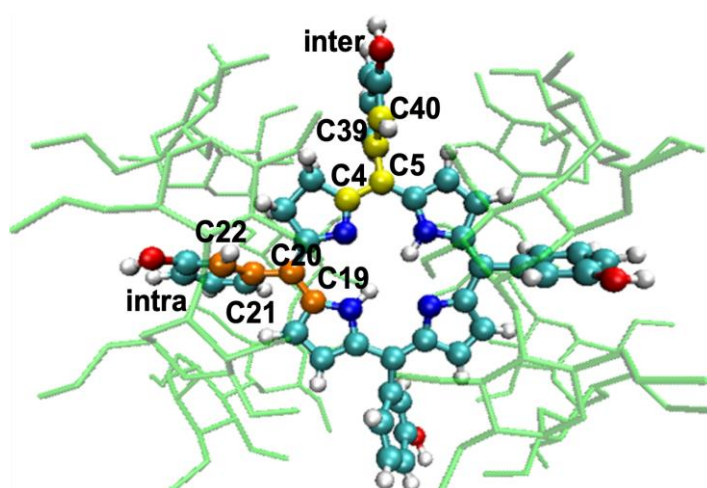


Figure S1. Dihedrals describing the orientation of the phenyl rings with respect to the chlorin ring and numbering used in the following.

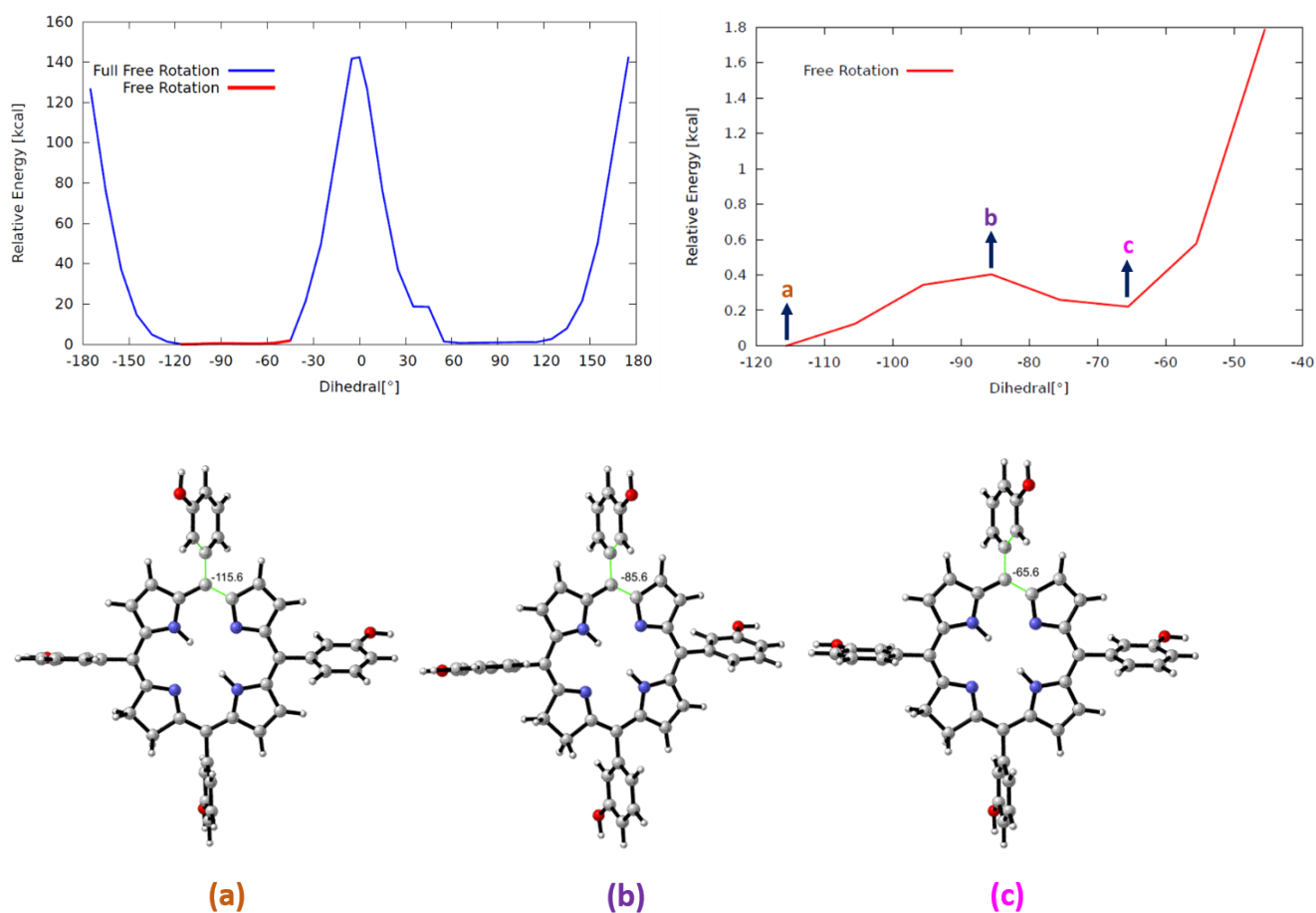


Figure S2. Top: rotational free energy (Mo62X/6-31+G(d)) profile for a dihedral scan (left hand side). On the right-hand side, a zoom of the region in red is shown. The geometry of the molecule in the three points a, b and c is displayed in the bottom panel.

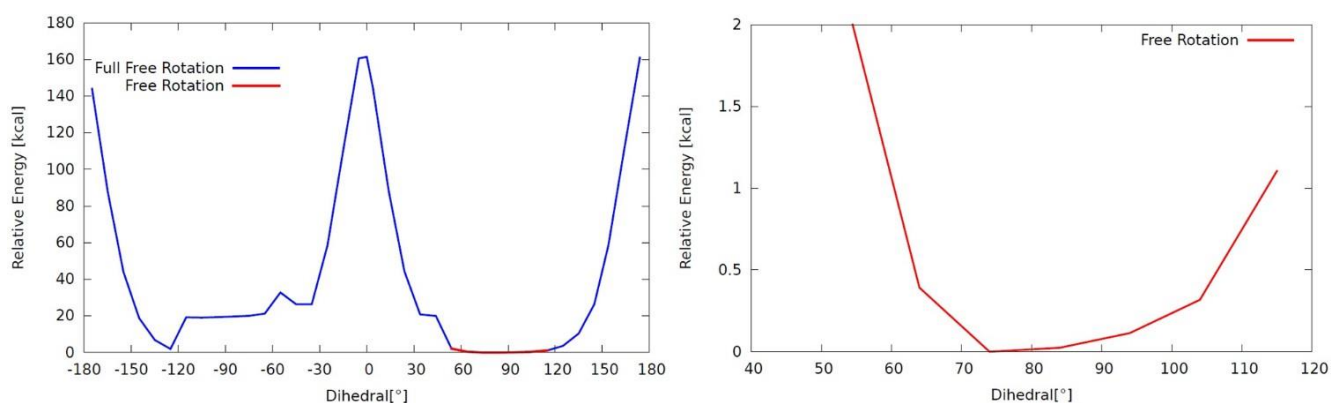


Figure S3. MP2/6-31G(d) energy profile along the rotation coordinate.

The most stable conformation of mTHPC is at -115° dihedral angles (structure a), Figure S2). As it can be seen in the zoom in Figure S2, the almost flat surface between -115° and -45° shows an almost free rotation of the ring in this region. The sharp maximum found at 0 and 180° is due to the steric clash

between the hydrogen atoms of the phenyl and porphyrin core. The maximum at -85.6° (structure b)) is correlated with a very small energy penalty of only 0.40 kcal/mol. Finally, the arrangement at -65.6° (structure c)) presents a slightly more energetic minimum, the difference in energy with structure a) being of only 0.22 kcal/mol. With this information in mind, we observed that the dihedral distribution obtained with oldFF gave a very poor agreement with the results from the quantum calculations (Figure S4).

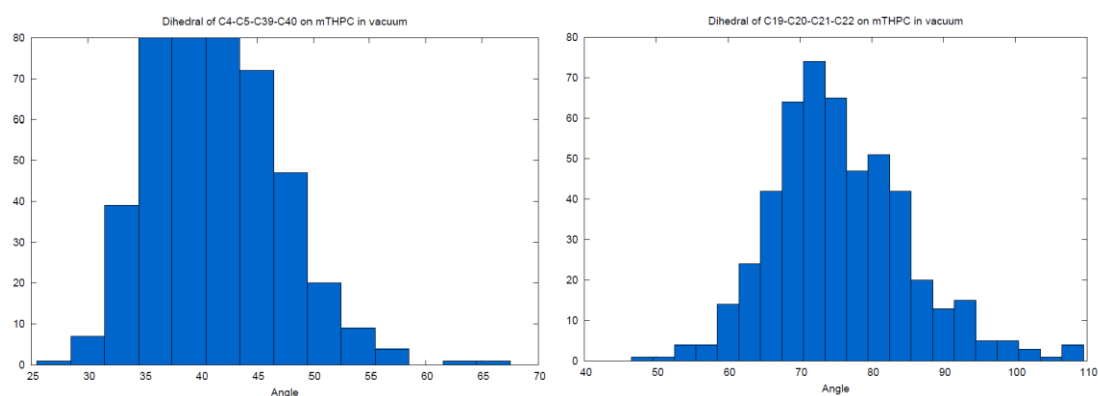


Figure S4. Distribution of the inter (left) and intra (right) dihedral angles during Simulation 2, carried out using oldFF.

A reparameterization of the dihedral potential was therefore necessary. Results obtained with the force field thus obtained (newFF) are reported in Figure S5 and compared with those obtained during Simulation 1.

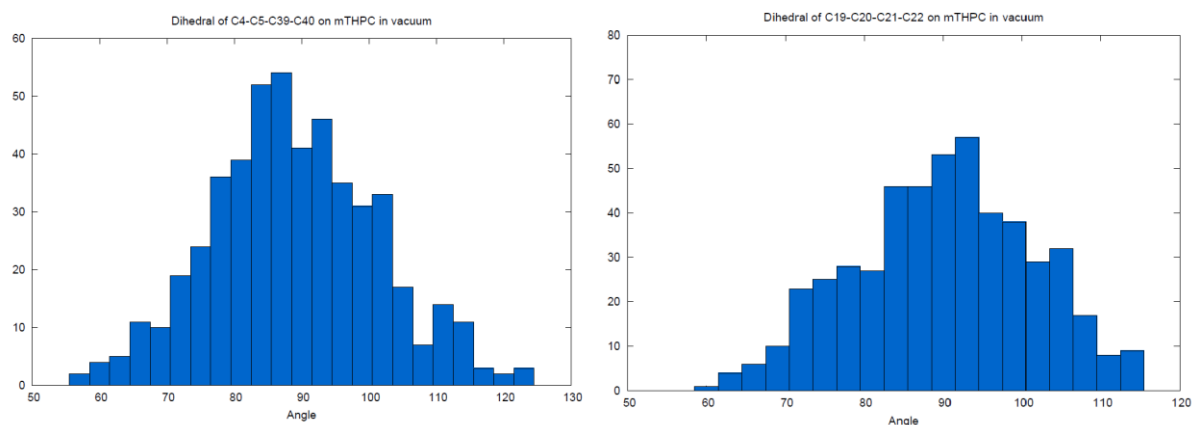


Figure S5. Distribution of the inter (left) and intra (right) dihedral angles during Simulation 3, carried out using newFF.

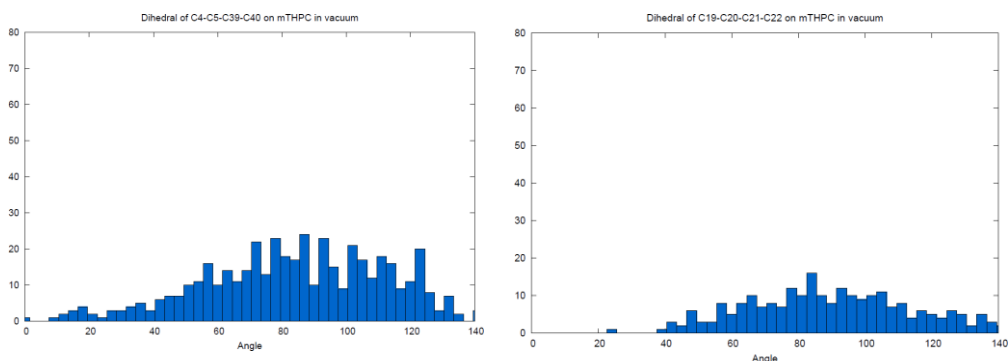


Figure S6. Distribution of the inter (left) and intra (right) dihedrals during Simulation 1.

The effects of the different parameterization on the optical properties determined for mTHPC were assessed by extracting 100 snapshots from Simulation 1, 2, and 3. The absorption spectrum was obtained as the convolution of the vertical transitions determined at Time Dependent Density Functional Theory¹² (TD-DFT). The level of theory was chosen following a benchmark in which vertical excitation energies are calculated for mTHPC at Franck-Condon geometry in implicit ethanol with B3LYP, Mo62X, and ω B97XD functionals as well as 6-31G, 6-31G(d), 6-31G(d,p), and 6-31G basissets as seen in Figure S7.

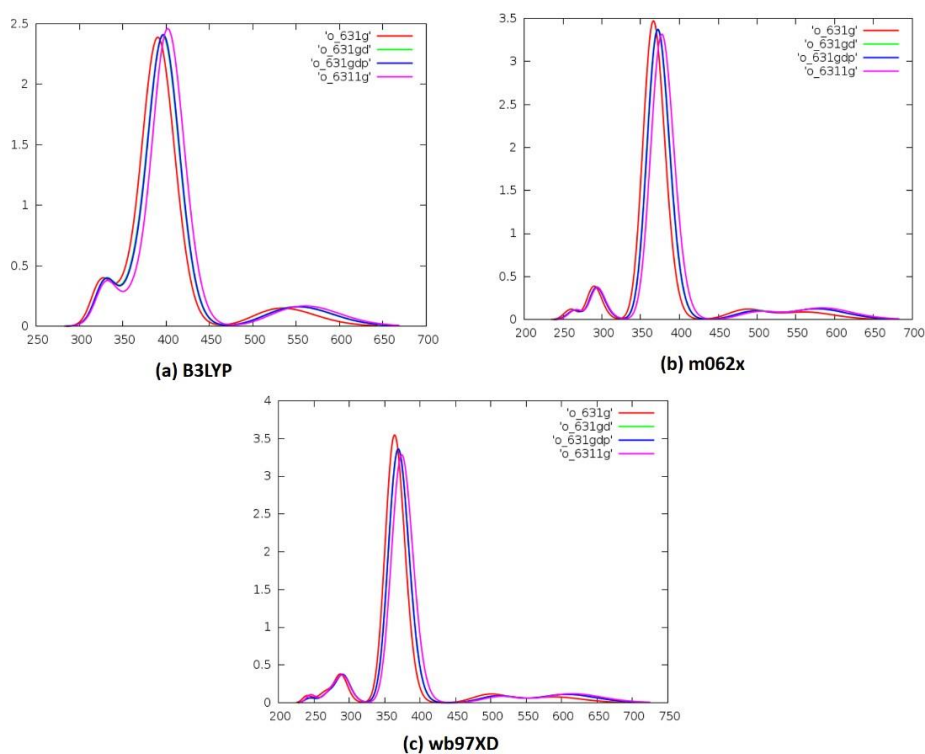


Figure S7. (a) B3LYP (b) Mo62X (c) \square B97XD absorption spectrum from the ground state equilibrium geometry. The bands are obtained convoluting the vertical transitions with gaussian functions of full-width at half-length of 0.3 eV.

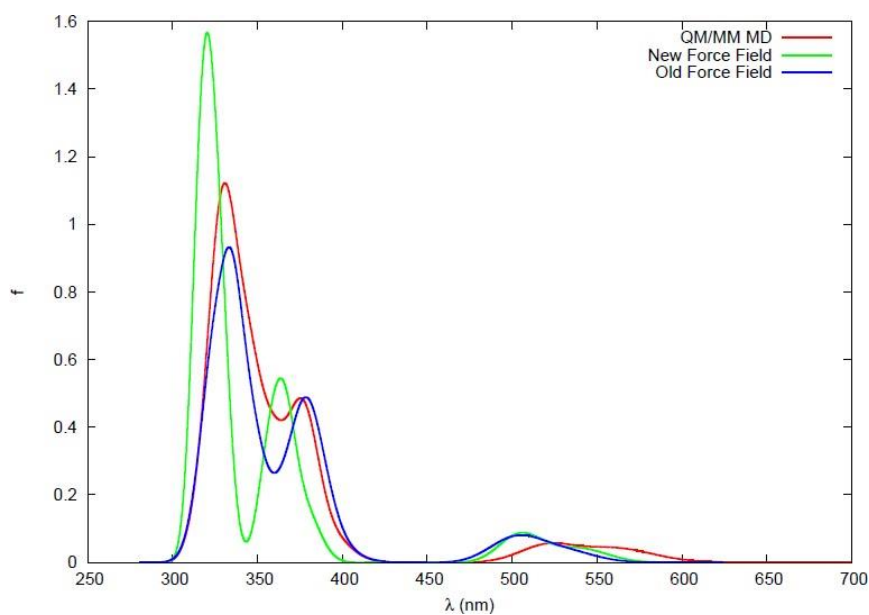


Figure S8. Absorption spectrum (B3LYP/6-31G) of isolated mTHPC obtained with Simulation 1 (QM/MM MD), 2 (oldFF) and 3 (newFF).

In Figure S9, we report the root mean square deviation (RMSD) obtained in the different simulations of the isolated molecule.

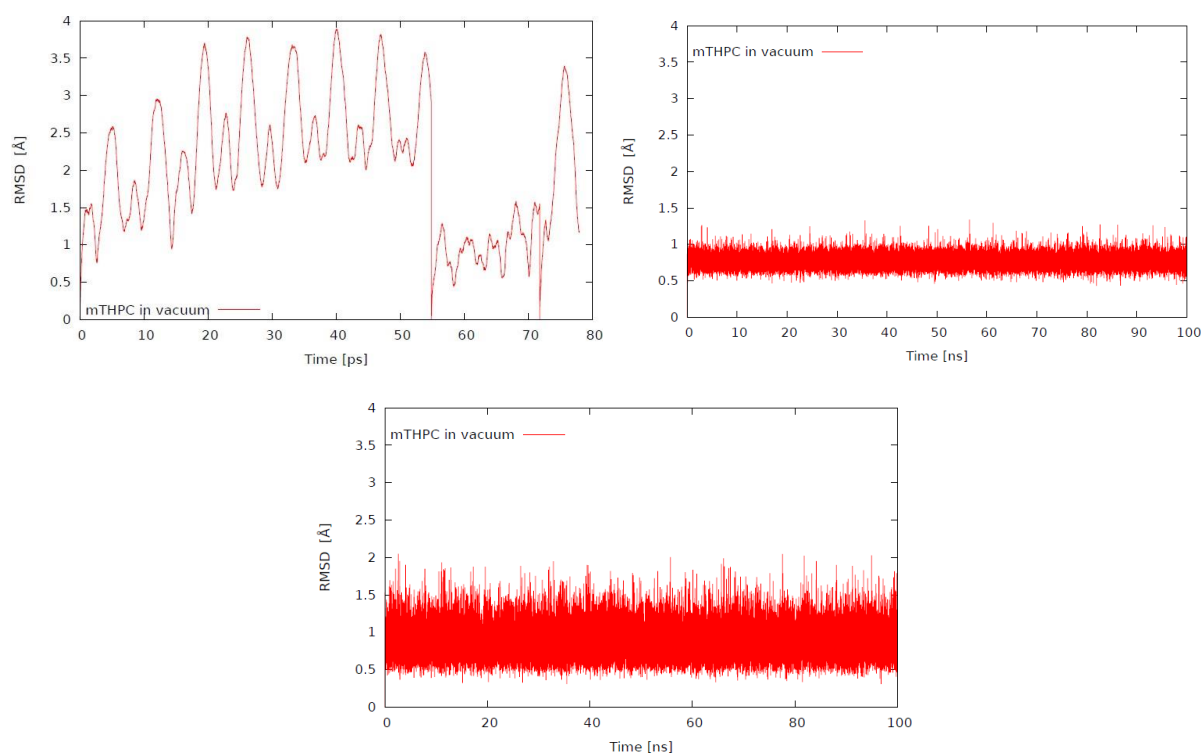


Figure S9. Root-Mean-Square-Deviation of isolated mTHPC in Simulation 1 (top left panel), 2 (top right panel) and 3 (bottom panel).

b) mTHPC in water

mTHPC was solvated in a water cubic box $50.0 \times 50.0 \times 50.0$ of 8 Angstrom using the TIP3P force field for water.¹³ The classical molecular dynamic simulations were performed using NAMD. Hybrid QM/MM MD¹⁴ calculations were done via the NAMD/Terachem interface for a total time of 50 ps. As in the preceding paragraph, we report in the following Figures the dihedral distribution, the absorption spectrum and the RMSD of the solute obtained for Simulations 1-3.

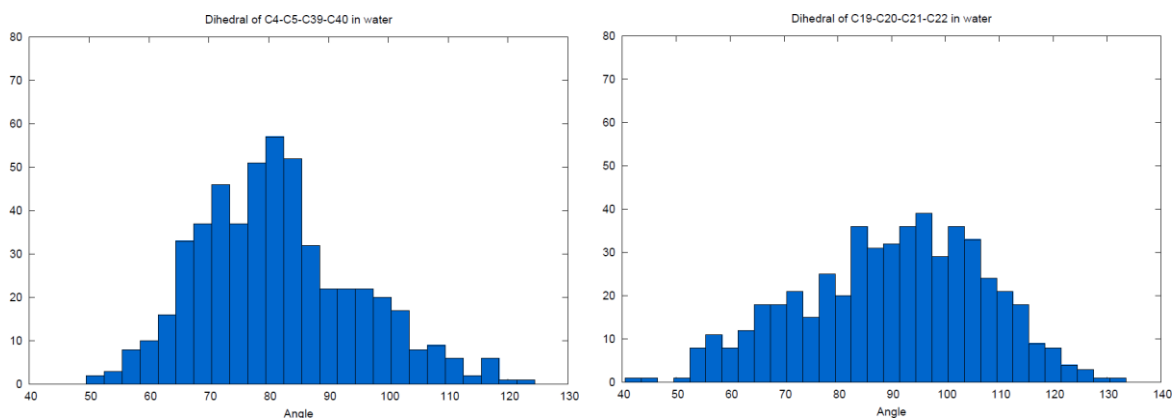


Figure S10. Distribution of the inter (left) and intra (right) dihedrals during Simulation 1.

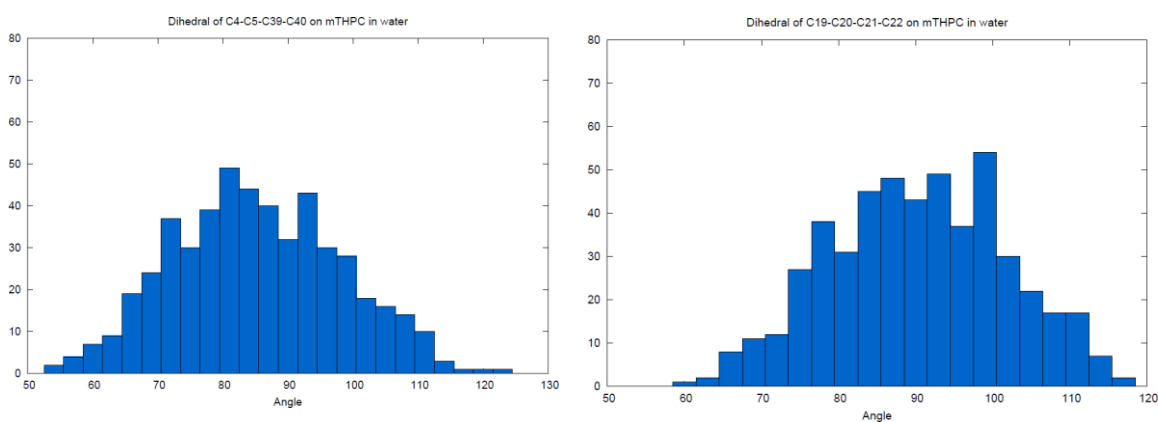


Figure S11. Distribution of the inter (left) and intra (right) dihedrals during Simulation 2, carried out using oldFF.

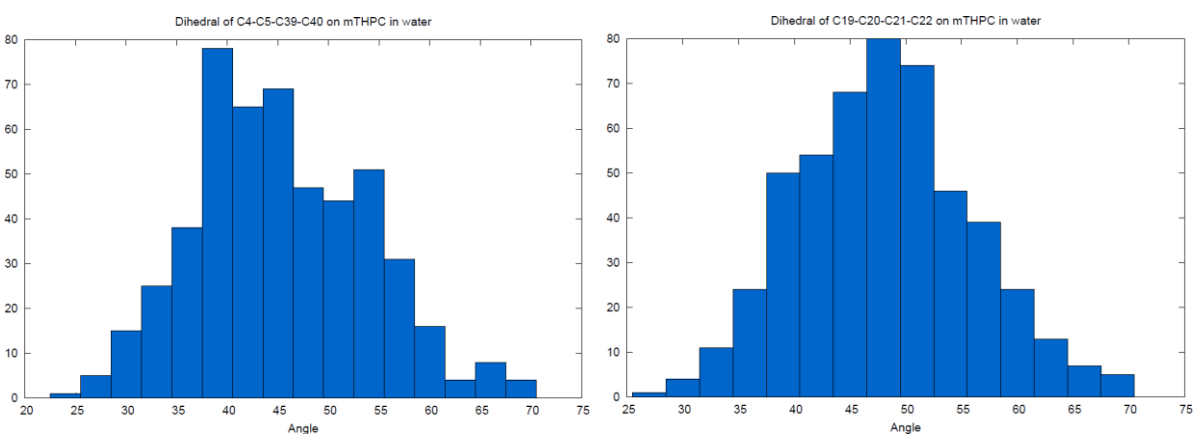
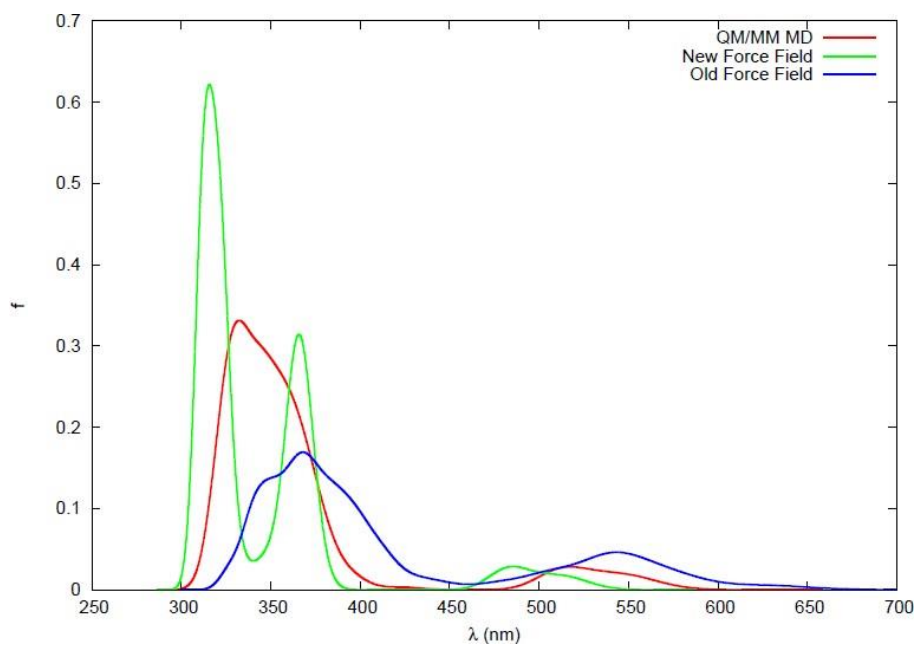
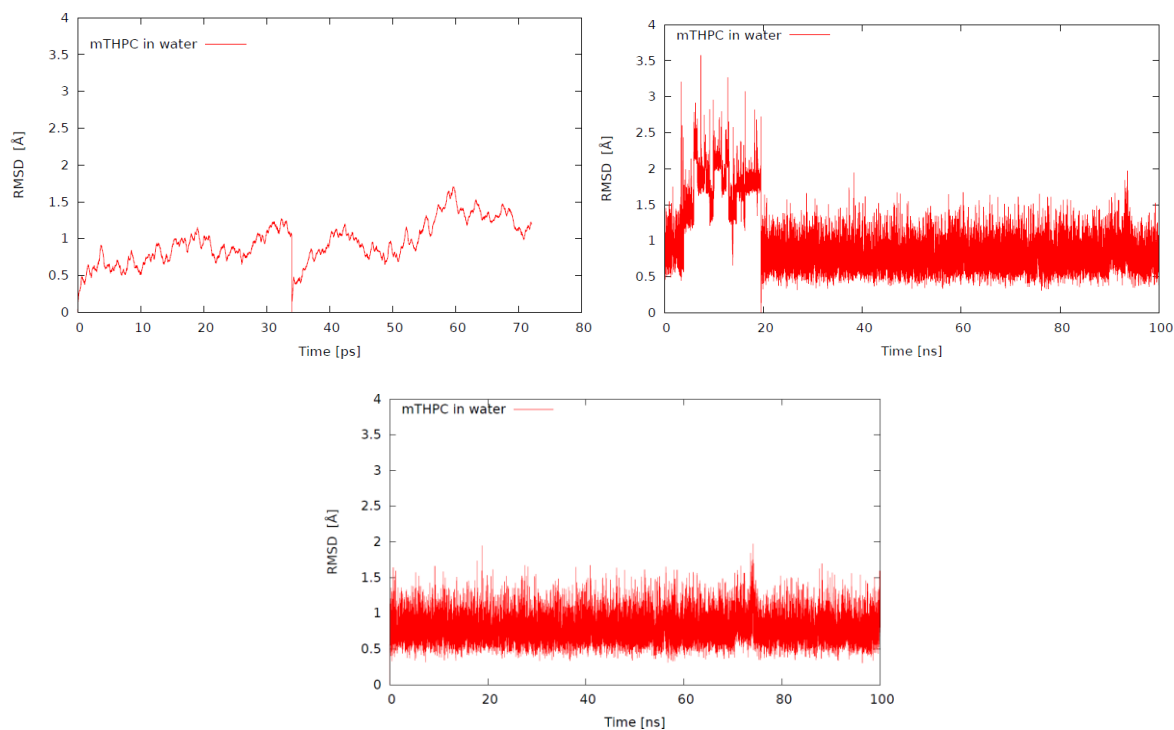


Figure S12. Distribution of the inter (left) and intra (right) dihedrals during Simulation 3, carried out using newFF.



FigureS13. Absorption spectrum of mTHPC in water (B₃LYP/6-31G) obtained with Simulation 1 (QM/MM MD), 2 (oldFF) and 3 (newFF).



FigureS14. Root-Mean-Square-Deviation of mTHPC in water in Simulation 1 (top left panel), 2 (top right panel) and 3 (bottom panel).

c) mTHPC:TM- β -CD complex

The host-guest complex formed by mTHPC with two cyclodextrins (TM- β -cyclodextrin) was also studied.¹⁵ The TM- β -cyclodextrin is described by the Amber GLYCAM force field,¹⁶ extending the parametrization of electrostatic charges according to a standard RESP^{17,18} protocol. Classic Molecular Dynamic simulations were carried out on one mTHPC encapsulated by two TM- β -CD and placed in 90.3x84.3x84.4 Angstrom water box modeled with TIP3P water model using the NAMD program package. Only simulations using newFF for mTHPC were performed (Simulation 3). Concerning Simulation 1, hybrid quantum mechanics/molecular mechanics (QM/MM) simulations were used to sample the conformational space of the complex and to determine the optical properties of the encapsulated chromophore. The hybrid QM/MM MD calculations for mTHPC:TM- β -CD complex were performed via TeraChem/Amber interface.¹⁹ Only the mTHPC molecule is placed into the QM partition, while TM- β -CD and the water molecules are treated as MM. The absorption spectra were calculated by convoluting vertical transitions from 100 snapshots taken from the hybrid QM/MM MD calculations and the classical MD simulations, the excited states are calculated with Terachem/Amber interface using the TD-DFT \square B97XD /6-31G method. In the following Figures, we report the dihedrals analysis and the RMSD computed for mTHPC and some relevant atoms describing the motions of the phenyl units and of the chlorin ring.

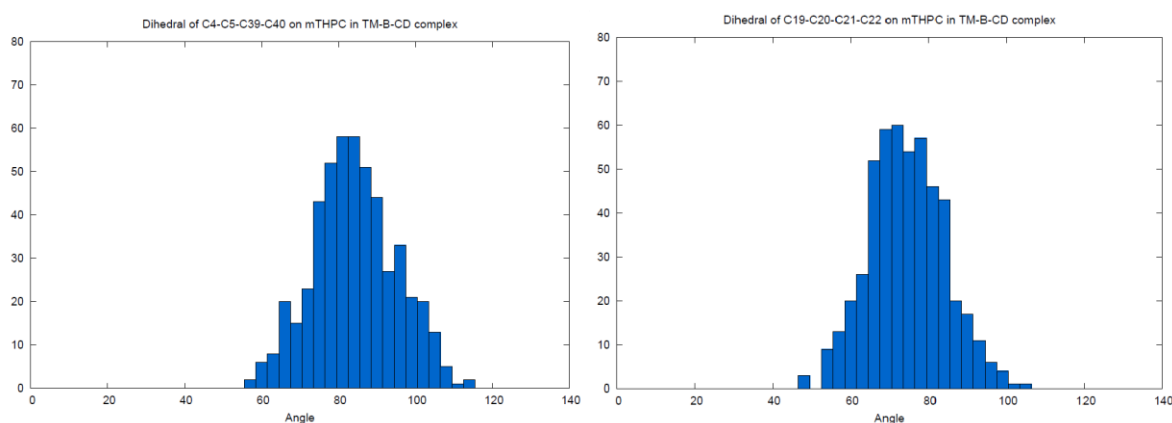


Figure S15. Distribution of the inter (left) and intra (right) dihedrals during Simulation 1.

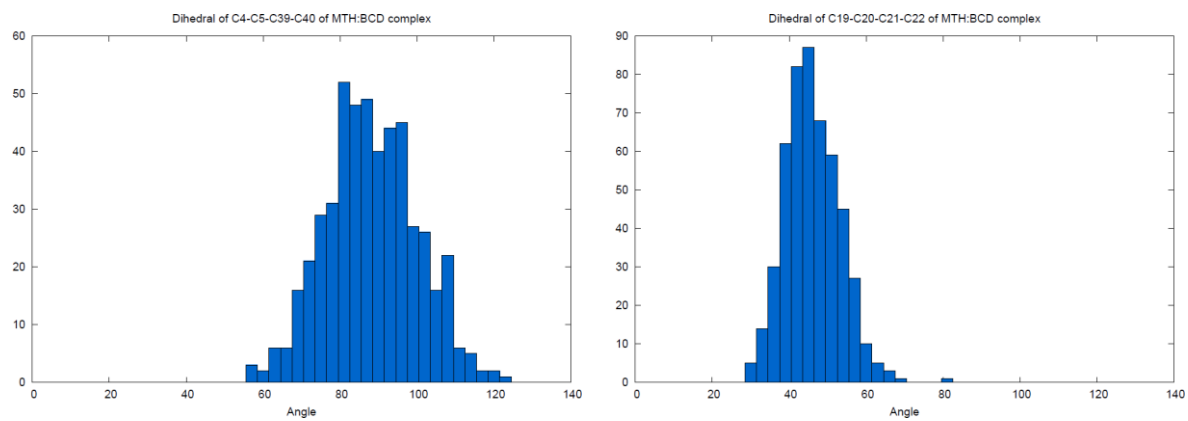


Figure S16. Distribution of the inter (left) and intra (right) dihedrals during Simulation 3.

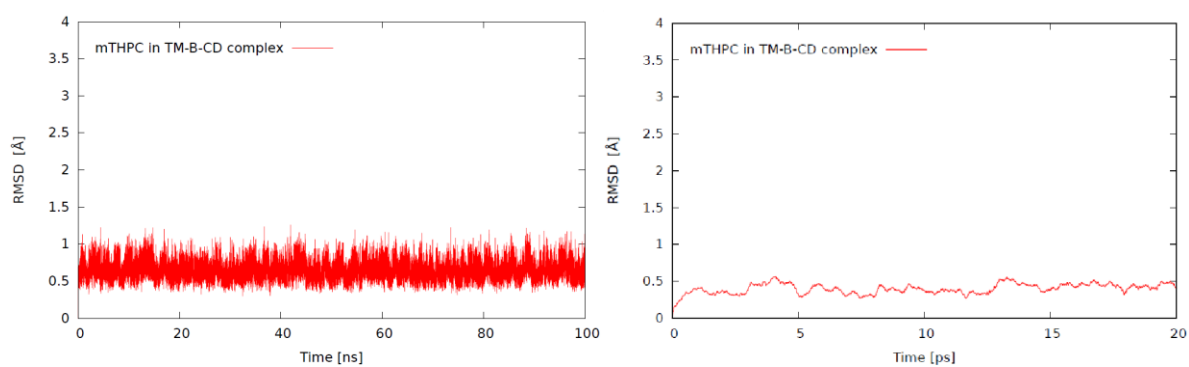


Figure S17. mTHPC TM- β -CD in water: Root-Mean-Square-Deviation of mTHPC in Simulation 1 (left panel) and 3 (right panel).

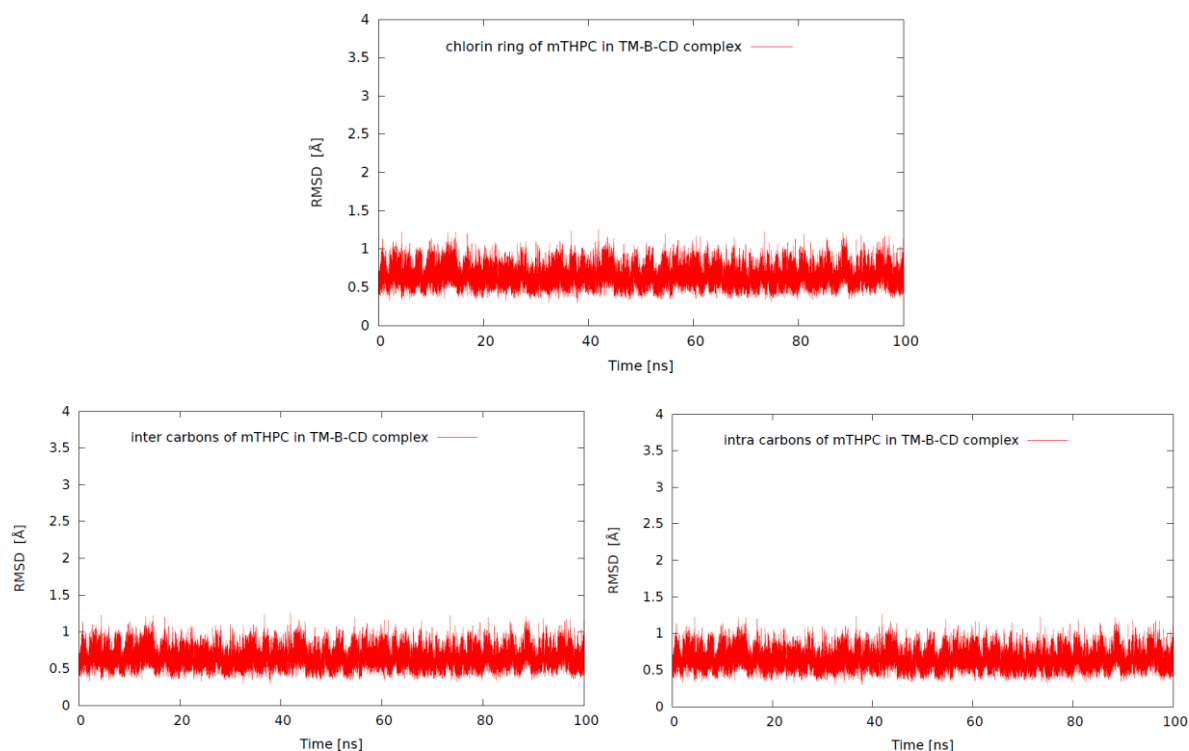


Figure S18. mTHPC:TM-β-CD in water: Root-Mean-Square-Deviation of in Simulation 3 for the chlorin ring (top panel), the inter carbons (bottom left panel) and the intra carbons (bottom right panel).

d) mTHPC interacting with a lipid POPC bilayer

In order to investigate the interaction of mTHPC with model biological complex systems, a POPC (1-palmitoyl-oleoyl-sn-glycero-phosphocholine) lipid bilayer was generated by the CHARMM-GUI Membrane Builder interface.^{20,21} Each leaflet includes 100 POPC chains and the membrane was solvated in water, and counter ions (K^+ , Cl^-) were added to mimic biological salt concentration. One mTHPC molecule was initially placed in the water bulk. Classical MD using newFF were exclusively carried out (Simulation 3). Since the very beginning of the simulation, it interacts persistently with the bilayer polar heads forming a stable aggregate over the 300 ns of the MD trajectory. The absorption spectrum of mTHPC was calculated using hybrid QM/MM protocol as described for water and cyclodextrin case. In the following Figures, we report the dihedral analysis as well as the RMSD of the molecule along the simulation.

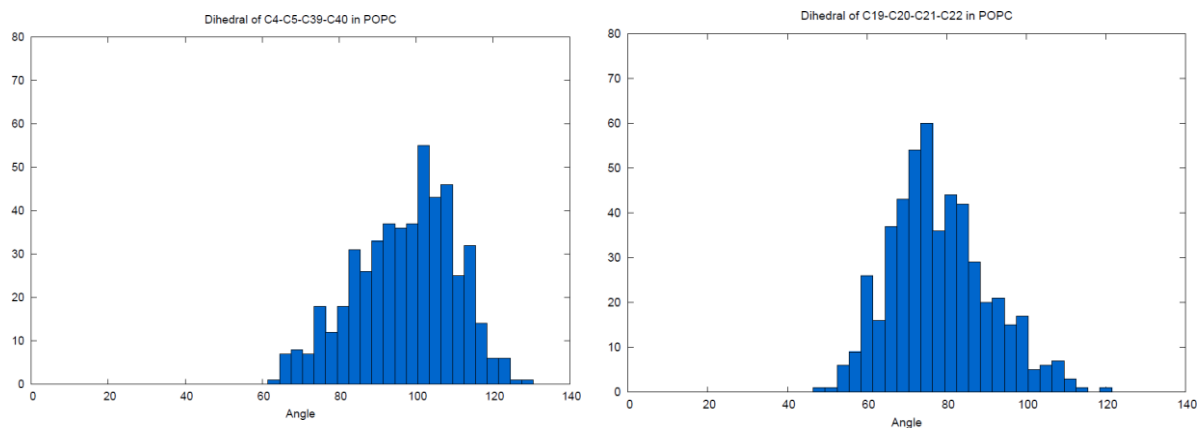


Figure S19. Distribution of the inter (left) and intra (right) dihedrals during Simulation 3.

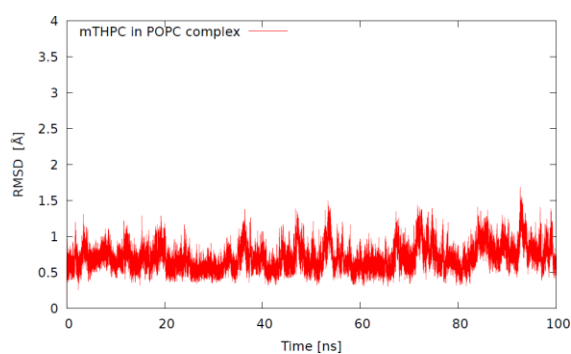


Figure S20. mTHPC interacting with a membrane: Root-Mean-Square-Deviation of in Simulation 3 for the mTHPC molecule.

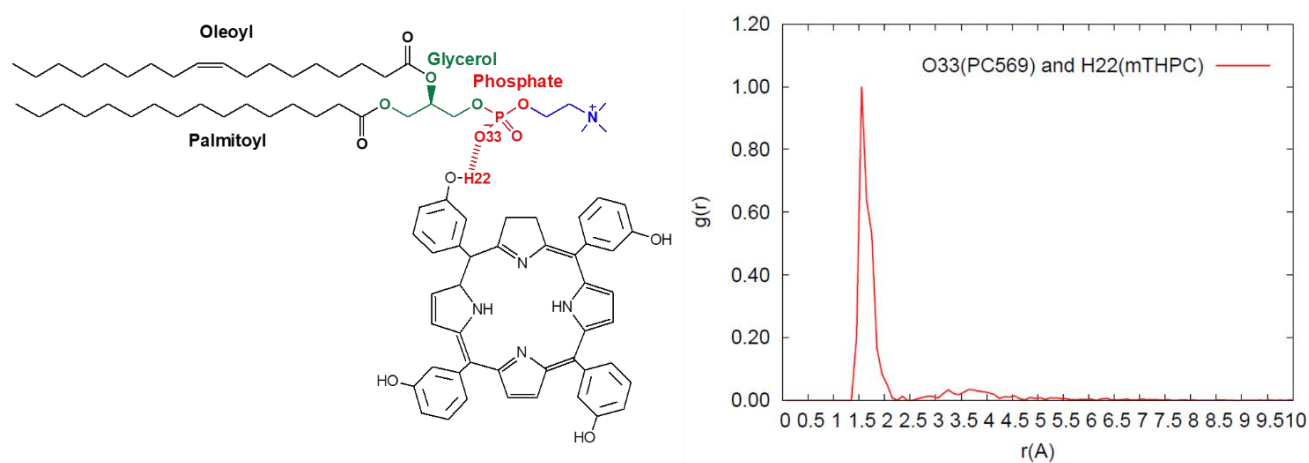


Figure S21. (left) 2D structure for the H-bond interaction between hydrogen of mTHPC and oxygen of POPC (right) radial pair distribution graph of this interaction collected from 100ns Classical MD simulation.

References

- (1) Lodola, A.; Mor, M.; Hermann, J. C.; Tarzia, G.; Piomelli, D.; Mulholland, A. J. QM/MM Modelling of Oleamide Hydrolysis in Fatty Acid Amide Hydrolase (FAAH) Reveals a New Mechanism of Nucleophile Activation. *Chem. Commun.* **2005**, No. 35, 4399–4401.
- (2) D.A. Case, R.M. Betz, D.S. Cerutti, T.E. Cheatham, III, T.A. Darden, R.E. Duke, T.J. Giese, H. G.; A.W. Goetz, N. Homeyer, S. Izadi, P. Janowski, J. Kaus, A. Kovalenko, T.S. Lee, S. LeGrand, P. Li, C.; Lin, T. Luchko, R. Luo, B. Madej, D. Mermelstein, K.M. Merz, G. Monard, H. Nguyen, H.T. Nguyen, I.; Omelyan, A. Onufriev, D.R. Roe, A. Roitberg, C. Sagui, C.L. Simmerling, W.M. Botello-Smith, J. S.; R.C. Walker, J. Wang, R.M. Wolf, X. Wu, L. Xiao and P.A. Kollman (2016), AMBER 2016, U. of; California, S. F. Amber 16.
- (3) Humphrey, W.; Dalke, A.; Schulten, K. VMD: Visual Molecular Dynamics. *J. Mol. Graph.* **1996**, *14* (1), 33–38, 27–28.
- (4) Hoover, W. G. Constant-Pressure Equations of Motion. *Phys. Rev. A* **1986**, *34* (3), 2499–2500.
- (5) Procacci, P.; Marsili, S.; Barducci, A.; Signorini, G. F.; Chelli, R. Crooks Equation for Steered Molecular Dynamics Using a No \acute{s} -Hoover Thermostat. *J. Chem. Phys.* **2006**, *125* (16).
- (6) Davidchack, R. L.; Handel, R.; Tretyakov, M. V. Langevin Thermostat for Rigid Body Dynamics. *J. Chem. Phys.* **2009**, *130* (23).
- (7) Wang, J.; Wolf, R. M.; Caldwell, J. W.; Kollman, P. A.; Case, D. A. Development and Testing of a General Amber Force Field. *J. Comput. Chem.* **2004**, *25* (9), 1157–1174.
- (8) Phillips, J. C.; Braun, R.; Wang, W. E. I.; Gumbart, J.; Tajkhorshid, E.; Villa, E.; Chipot, C.; Skeel, R. D.; Poincare, H. Scalable Molecular Dynamics with NAMD. **2005**.
- (9) Stephens, P. J.; Devlin, F. J.; Chabalowski, C. F.; Frisch, M. J. Ab Initio Calculation of Vibrational Absorption and Circular Dichroism Spectra Using Density Functional Force Fields. *J. Phys. Chem.* **1994**, *98* (45), 11623–11627.
- (10) Frisch, M. J.; Trucks, G. W.; Schlegel, H. B.; Scuseria, G. E.; Robb, M. A.; Cheeseman, J. R.; Scalmani, G.; Barone, V.; Mennucci, B.; Petersson, G. A.; Nakatsuji, H.; Caricato, M.; Li, X.; Hratchian, H. P.; Izmaylov, A. F.; Bloino, J.; Zheng, G.; Sonnenb, W. C. Gaussian 09, Revision A.02. **2009**.
- (11) Frisch, M. J.; Trucks, G. W.; Schlegel, H. B.; Scuseria, G. E.; Robb, M. A.; Cheeseman, J. R.; Scalmani, G.; Barone, V.; Petersson, G. A.; Nakatsuji, H.; Li, X.; Caricato, M.; Marenich, A. V.; Bloino, J.; Janesko, B. G.; Gomperts, R.; Mennucci, B.; Hratch. Gaussian 16, Revision C.01. **2016**.
- (12) Stratmann, R. E.; Scuseria, G. E.; Frisch, M. J. An Efficient Implementation of Time-Dependent Density-Functional Theory for the Calculation of Excitation Energies of Large Molecules. *J. Chem. Phys.* **1998**, *109* (19), 8218–8224.
- (13) Mark, P.; Nilsson, L. Structure and Dynamics of the TIP3P, SPC, and SPC/E Water Models at 298 K. *J. Phys. Chem. A* **2001**, *105* (43), 9954–9960.
- (14) Sgrignani, J.; Magistrato, A. QM/MM MD Simulations on the Enzymatic Pathway of the Human Flap Endonuclease (HFEN1) Elucidating Common Cleavage Pathways to RNase H Enzymes. *ACS Catal.* **2015**, *5* (6), 3864–3875.
- (15) Yakavets, I.; Lassalle, H. P.; Scheglmann, D.; Wiehe, A.; Zorin, V.; Bezdetnaya, L. Temoporfin-in- Cyclodextrin-in-Liposome—a New Approach for Anticancer Drug Delivery: The Optimization of Composition. *Nanomaterials* **2018**, *8* (10), 1–15.
- (16) Uhe, A.; Kozuch, S.; Shaik, S. Software News and Update Automatic Analysis of Computed Catalytic Cycles. *J. Comput. Chem.* **2010**, 1–8.

- (17) Bayly, C. I.; Cieplak, P.; Cornell, W. D.; Kollman, P. A. A Well-Behaved Electrostatic Potential Based Method Using Charge Restraints for Deriving Atomic Charges: The RESP Model. *J. Phys. Chem.* **1993**, *97* (40), 10269–10280.
- (18) Cornell, W. D.; Cieplak, P.; Bayly, C. I.; Kollman, P. A. Application of RESP Charges To Calculate

- Conformational Energies, Hydrogen Bond Energies, and Free Energies of Solvation. *J. Am. Chem. Soc.* **1993**, *115* (21), 9620–9631.
- (19) Titov, A. V.; Ufimtsev, I. S.; Luehr, N.; Martinez, T. J. Generating Efficient Quantum Chemistry Codes for Novel Architectures. *J. Chem. Theory Comput.* **2013**, *9* (1), 213–221.
- (20) Wu, E. L.; Cheng, X.; Jo, S.; Rui, H.; Song, K. C.; Dávila-Contreras, E. M.; Qi, Y.; Lee, J.; Monje-Galvan, V.; Venable, R. M.; et al. CHARMM-GUI Membrane Builder toward Realistic Biological Membrane Simulations. *Journal of Computational Chemistry*. October 2014, pp 1997–2004.
- (21) Jo, S.; Lim, J. B.; Klauda, J. B.; Im, W. CHARMM-GUI Membrane Builder for Mixed Bilayers and Its Application to Yeast Membranes. *Biophys. J.* **2009**, *97* (1), 50–58.

Cartesian Coordinates of mTHPC in QM MD

C 12.8190000000 -27.6620000000 -29.3490000000

C 14.3400000000 -27.4950000000 -29.2090000000
C 14.5870000000 -26.0900000000 -29.7600000000
N 13.4270000000 -25.4720000000 -30.1390000000
C 12.3720000000 -26.3110000000 -29.9100000000
C 11.0260000000 -26.0200000000 -30.1140000000
C 10.4960000000 -24.8110000000 -30.6040000000
C 9.1000000000 -24.5100000000 -30.7770000000
C 8.9930000000 -23.2340000000 -31.2830000000
C 10.3170000000 -22.7050000000 -31.4560000000
N 11.1940000000 -23.6960000000 -31.0200000000
C 10.6730000000 -21.4560000000 -31.9710000000
C 11.9920000000 -20.9770000000 -32.1150000000
C 12.3250000000 -19.7110000000 -32.7580000000
C 13.6850000000 -19.6040000000 -32.7380000000
C 14.1910000000 -20.8020000000 -32.0780000000
N 13.1450000000 -21.6330000000 -31.7170000000
C 15.5640000000 -21.0580000000 -31.8690000000
C 16.0930000000 -22.2210000000 -31.3050000000
C 17.4720000000 -22.4970000000 -31.0060000000
C 17.5480000000 -23.7510000000 -30.4440000000
C 16.2190000000 -24.2960000000 -30.3720000000
C 15.8720000000 -25.5590000000 -29.8540000000
C 17.0090000000 -26.4110000000 -29.3700000000
C 17.2720000000 -26.5230000000 -28.0000000000
C 18.3230000000 -27.3270000000 -27.5490000000
C 19.1290000000 -28.0230000000 -28.4580000000
C 18.8690000000 -27.9070000000 -29.8280000000
C 17.8180000000 -27.1080000000 -30.2860000000
O 18.5190000000 -27.3870000000 -26.1720000000
N 15.3730000000 -23.3420000000 -30.8950000000
C 16.5450000000 -20.0060000000 -32.2780000000
C 17.4800000000 -20.2700000000 -33.2880000000
C 18.4000000000 -19.2890000000 -33.6670000000
C 18.4040000000 -18.0360000000 -33.0450000000
C 17.4700000000 -17.7720000000 -32.0370000000
C 16.5450000000 -18.7450000000 -31.6520000000

O 19.2880000000 -19.6280000000 -34.6850000000
C 9.5500000000 -20.5750000000 -32.4200000000
C 9.3040000000 -19.3580000000 -31.7710000000
C 8.2490000000 -18.5430000000 -32.1890000000
C 7.4310000000 -18.9230000000 -33.2580000000
C 7.6820000000 -20.1350000000 -33.9100000000
C 8.7320000000 -20.9590000000 -33.5000000000
O 8.0580000000 -17.3570000000 -31.4830000000
C 10.0280000000 -27.0880000000 -29.7740000000
C 9.3620000000 -27.0680000000 -28.5410000000
C 8.4400000000 -28.0710000000 -28.2270000000
C 8.1690000000 -29.1010000000 -29.1330000000
C 8.8310000000 -29.1190000000 -30.3650000000
C 9.7540000000 -28.1220000000 -30.6890000000
O 7.8230000000 -27.9830000000 -26.9820000000
H 12.5430000000 -28.4740000000 -30.0300000000
H 12.3220000000 -27.8720000000 -28.3960000000
H 14.6770000000 -27.5710000000 -28.1700000000
H 14.9090000000 -28.2380000000 -29.7770000000
H 8.3000000000 -25.1880000000 -30.5320000000
H 8.0880000000 -22.6970000000 -31.5150000000
H 12.2000000000 -23.5860000000 -31.0030000000
H 11.6130000000 -19.0190000000 -33.1790000000
H 14.2900000000 -18.8080000000 -33.1400000000
H 18.2840000000 -21.8150000000 -31.1940000000
H 18.4320000000 -24.2620000000 -30.0980000000
H 16.6750000000 -25.9840000000 -27.2750000000
H 19.9450000000 -28.6460000000 -28.1030000000
H 19.4930000000 -28.4420000000 -30.5360000000
H 17.6170000000 -27.0180000000 -31.3480000000
H 19.2810000000 -27.9530000000 -25.9410000000
H 14.3640000000 -23.4130000000 -30.9540000000
H 17.4940000000 -21.2270000000 -33.7950000000
H 19.1220000000 -17.2760000000 -33.3420000000
H 17.4710000000 -16.8040000000 -31.5480000000
H 15.8260000000 -18.5400000000 -30.8670000000
H 19.8830000000 -18.8850000000 -34.9040000000
H 9.9160000000 -19.0400000000 -30.9370000000

H 6.6130000000 -18.2850000000 -33.5790000000
H 7.0560000000 -20.4320000000 -34.7450000000
H 8.9300000000 -21.8940000000 -34.0100000000
H 7.2960000000 -16.8540000000 -31.8270000000
H 9.5520000000 -26.2820000000 -27.8220000000
H 7.4500000000 -29.8780000000 -28.8840000000
H 8.6200000000 -29.9130000000 -31.0740000000
H 10.2600000000 -28.1290000000 -31.6490000000
H 7.2000000000 -28.7200000000 -26.8360000000

Cartesian Coordinates for mTHPC:TM- β -CD in water in QM/MM MD

C 3.0074440260 2.6359999623 -2.0245655446
C 3.9423030886 1.8683820927 -1.0798395045
C 2.8585235900 1.0327814192 -0.2255752433
N 1.5977908876 1.2715968670 -0.6783651318
C 1.5464858445 2.1607506667 -1.6913527196
C 0.4476787036 2.7089319588 -2.3053752718
C -0.8761228087 2.2085371791 -2.0972353379
C -2.0441754164 2.7792722727 -2.7237564425
C -3.1645630537 2.1020688085 -2.2941221263
C -2.6990691335 1.1020491817 -1.2991261068
N -1.2978021916 1.2633175835 -1.2240284212
C -3.3730832908 0.0539706209 -0.6537917756
C -2.8158829868 -0.9523867038 0.2258375830
C -3.8134846388 -1.9857487619 0.7856136808
C -3.0606233840 -2.7067047112 1.7106680978
C -1.6653047017 -2.1560403733 1.6073108601
N -1.5491086088 -1.1160941301 0.7441766667
C -0.4887939742 -2.6728750963 2.3396832564
C 0.8079580577 -2.2071563938 2.1920540724
C 1.9678970002 -2.7321452900 2.7387695586
C 3.0325884388 -1.9195582604 2.3304650537
C 2.5250748051 -0.8767234542 1.4613723369
C 3.2915661794 0.1215107845 0.7294057447

C 4.8206259157 0.0740244283 1.1379815864
C 5.5607478269 -0.9968708835 0.7248582962
C 6.9069729349 -1.0324347656 1.0062233267
C 7.5610292325 0.0900675271 1.6381270914
C 6.8087689145 1.1587129293 1.9646627753
C 5.4253149732 1.1422826995 1.7082056741
O 7.4827302408 -2.1653063001 0.5945796910
N 1.1947118840 -1.1643195182 1.3443003584
C -0.6174913584 -3.9839243057 3.1501737978
C -0.9437321965 -3.9036828011 4.4949188758
C -0.8896269422 -4.9570452102 5.3151785281
C -0.6873831197 -6.1933722408 4.7612870670
C -0.5272574035 -6.3464637121 3.4480761713
C -0.5750917144 -5.2791947055 2.5646656208
O -1.0729844762 -4.7199519008 6.7344345020
C -4.8150528348 -0.0298593793 -1.0711248396
C -5.2423762785 -0.8056773928 -2.1327323526
C -6.6211810291 -0.8481461759 -2.4258493036
C -7.5092215632 -0.0371645784 -1.7075500112
C -7.0472154186 0.9492568285 -0.8818328545
C -5.6859533246 0.8332003439 -0.5132907953
O -6.9508176689 -1.6757544973 -3.4738041736
C 0.7218513625 3.8696568839 -3.2374505358
C 1.1987263573 3.6323527377 -4.4926271586
C 1.3639800370 4.6847771506 -5.4361611167
C 1.3357118807 6.0247962994 -5.0013739308
C 1.0034522674 6.3882119232 -3.6520463699
C 0.6880034435 5.3053393382 -2.7541190457
O 1.6460161482 4.3760736444 -6.7829761498
H 3.1327812304 3.6760005619 -1.7904883164
H 3.0899021574 2.6268524589 -3.0832939554
H 4.6529713109 1.2366709114 -1.6121729137
H 4.5252337091 2.4840985225 -0.3705473639
H -2.1717798597 3.6515172468 -3.3138600655

H -4.2067785406 2.2599936260 -2.5287909201
H -0.6706212418 0.7522791554 -0.5477683829
H -4.8340111469 -2.1869705069 0.3688256026
H -3.4626816832 -3.5685724214 2.2841302221
H 1.9278984092 -3.4761966435 3.5309879375
H 4.0639846032 -2.0506954991 2.5749227658
H 5.0919641442 -1.8371368106 0.2363992090
H 8.6022048107 -0.0634935322 1.9887841579
HH 7.1692163102 1.8690168362 2.8226089684
4.8741900459 2.0199312791 2.0307347483
H 8.3657325720 -2.4309088831 0.8514241935
H 0.5759670549 -0.6415110287 0.7735808833
H -1.2627129957 -2.9109928463 4.7930727095
H -0.6224562279 -7.0520505750 5.3567233196
H -0.5899361579 -7.3959927735 3.0198227705
H -0.4923174025 -5.2980238180 1.4483595010
H -1.5956853081 -5.4647383903 7.1409386283
H -4.6586764509 -1.4051687259 -2.8004320813
H -8.6022048107 -0.0174641654 -1.9340104718
H -7.5896828685 1.7922251913 -0.5608958318
H -5.3373497043 1.6247798625 0.1191747419
H -7.7593284887 -1.4700140836 -4.0219080709
H 1.0095480248 2.5784733001 -4.8169177119
H 1.4804516370 6.8276085314 -5.7261953467
H 0.9237200345 7.3959927735 -3.2329130970
H 0.4263412030 5.4368734143 -1.7727366533
H 2.3915452382 4.9327639747 -7.1409386283

